

# Semi-Supervised Domain Adaptation via Adaptive and Progressive Feature Alignment

Jiaxing Huang, Dayan Guan, Aoran Xiao, Shijian Lu\*  
 School of Computer Science Engineering, Nanyang Technological University  
 {Jiaxing.Huang, Dayan.Guan, Aoran.Xiao, Shijian.Lu}@ntu.edu.sg

## Abstract

Contemporary domain adaptive semantic segmentation aims to address data annotation challenges by assuming that target domains are completely unannotated. However, annotating a few target samples is usually very manageable and worthwhile especially if it improves the adaptation performance substantially. This paper presents SSDAS, a Semi-Supervised Domain Adaptive image Segmentation network that employs a few labeled target samples as anchors for adaptive and progressive feature alignment between labeled source samples and unlabeled target samples. We position the few labeled target samples as references that gauge the similarity between source and target features and guide adaptive inter-domain alignment for learning more similar source features. In addition, we replace the dissimilar source features by high-confidence target features continuously during the iterative training process, which achieves progressive intra-domain alignment between confident and unconfident target features. Extensive experiments show the proposed SSDAS greatly outperforms a number of baselines, i.e., UDA-based semantic segmentation and SSDA-based image classification. In addition, SSDAS is complementary and can be easily incorporated into UDA-based methods with consistent improvements in domain adaptive semantic segmentation.

## 1. Introduction

Domain adaptation has been investigated extensively for the task of semantic segmentation, largely for minimizing the gap between a labeled source domain (typically consisting of synthetic images with automatically generated labels) and an unlabeled target domain and accordingly alleviating the pain point of pixel-level annotation of large amounts of training images. Most existing domain adaptive semantic segmentation works are unsupervised [21, 28, 29, 44, 47, 49, 35, 51, 6, 7] which assume

\*Corresponding author.

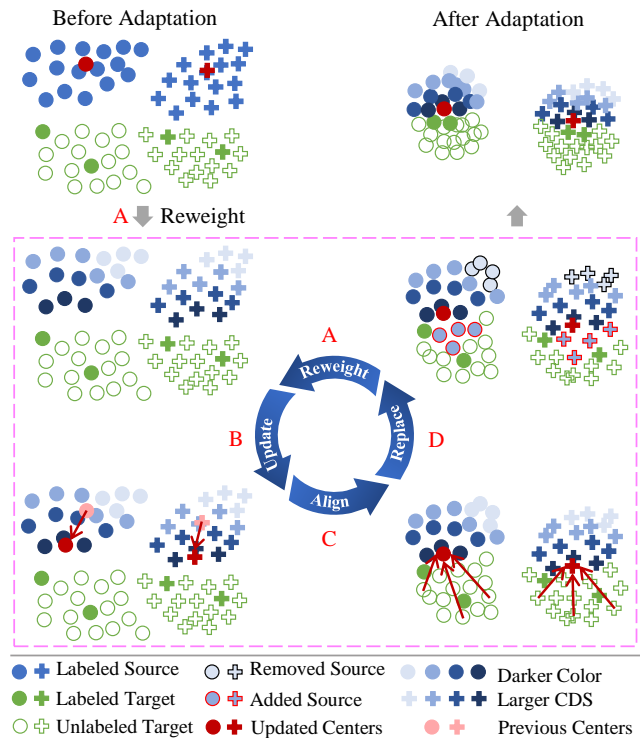


Figure 1. Illustration of our proposed semi-supervised domain adaptive semantic segmentation (SSDAS): With a few labeled target samples as anchors, SSDAS achieves semi-supervised domain adaptation via 4 key processes including **A**: re-weight source features according to their similarity to the feature of the few labeled target samples, *i.e.*, cross-domain similarity (CDS), **B**: update feature centers with newly weighted source features, **C**: align target features to the updated feature centers, and **D**: replace dissimilar source features by high-confidence target features. The four processes run iteratively which keep assigning higher weights to target-alike source features and replacing target-unlike source features with confident target features adaptively and progressively (Best viewed in color).

a completely unannotated target domain. However, annotating a few target samples is often very manageable and worthwhile especially if it can substantially improve the

segmentation performance in the target domain. By managing the amount of labeling in the target domain flexibly, such semi-supervised domain adaptation (SSDA) is also more scalable while facing very diverse domain gaps where unsupervised domain adaptation (UDA) often fails to handle well (e.g. when the domain gap is very large).

SSDA based semantic segmentation has been largely neglected despite its great values in various practical tasks. One intuitive approach to this new problem is to adapt existing UDA methods by including extra supervision from the few labeled target samples in the training process. However, existing UDA methods were designed without considering few-shot labelling in the semi-supervised setup, and recent studies [40, 30] show that this intuitive approach does not perform clearly better (sometimes even worse) than direct training over all labeled source and few-shot target samples in a supervised manner. Considering the similarity between semantic segmentation and image classification, another approach is to adapt the recent SSDA based image classification methods [40, 30] for the semantic segmentation problem. However, the SSDA based image classification methods do not perform well for the dense prediction of image pixels which often experiences much larger and more diverse variations across domains.

We propose SSDAS, a Semi-Supervised Domain Adaptive Segmentation network that positions a few labeled target samples as anchors for effective feature alignment between labeled source samples and unlabeled target samples. We introduce two novel designs for optimal feature alignment across domains. The first design is *adaptive cross-domain alignment* that takes the few labeled target samples as references to gauge the cross-domain similarity (CDS) of each source feature and learn more from target-alike source features. Specifically, we raise (or lower) the weight of source features that are similar (or dissimilar) to the target features adaptively during the domain adaptation process as illustrated in Fig. 1. The second design is *progressive intra-domain alignment* where target-unlike source features are replaced by high-confidence target features progressively and the alignment becomes in-between confident and unconfident target features. The proposed SSDAS adopts Jigsaw Puzzle classifiers to extract contextual features for domain adaptive semantic segmentation and it can also work with conventional features, more details to be discussed in experiments.

The contributions of this work can be summarized in three major aspects. *First*, we design SSDAS – an innovative semi-supervised domain adaptive segmentation network that exploits a few labeled target samples for better domain adaptive semantic segmentation. To the best of our knowledge, this is the first work that explores semi-supervised domain adaptation (with few-shot labels) for the classical semantic segmentation task. *Second*, we design

two novel feature alignment strategies for semi-supervised domain adaptation problems. The strategies exploit a few labeled target samples and achieve adaptive cross-domain alignment and progressive intra-domain alignment effectively. *Third*, extensive experiments over multiple domain adaptive segmentation tasks show that our proposed SSDAS achieves superior semantic segmentation consistently.

## 2. Related Works

**Unsupervised Domain Adaptation (UDA)** has been studied extensively for the task of semantic segmentation. Existing UDA-based segmentation methods can be broadly classified into three categories. The first category is *adversarial training* based which utilizes a domain classifier to align source and target distributions in the feature, output or latent space [21, 34, 49, 35, 47, 8, 56, 41, 42, 51, 48, 32, 18, 54, 23]. The second category is *image translation* based which translates images from source to target domains to mitigate domain gaps [20, 44, 9, 33, 55, 22, 52, 25]. The third category is *self-training* based which utilizes “pseudo labels” to guide iterative learning over unlabeled target data [59, 43, 57, 58, 17, 24].

**Semi-supervised Domain Adaptation (SSDA)** assumes the availability of a few labeled target samples beyond labeled source samples and a large amount of unlabeled target samples as in UDA. Several SSDA methods [1, 13, 53, 40, 30, 27] have been proposed which addresses domain discrepancy by auxiliary constrain optimization [13], subspace learning [53], label smoothing [1], entropy minimax [40], intra-domain discrepancy minimization [30] and bidirectional adversarial training [27]. However, most existing SSDA works focus on image classification and the relevant semantic segmentation task involving dense pixel-level predictions is largely neglected. We focus on SSDA-based semantic segmentation (with few-shot target samples) and it is the first effort for this challenging task to the best of our knowledge.

**Jigsaw Puzzles** is a basic pattern recognition problem that aims to reconstruct an original image from its shuffled patches. In the field of computer science and artificial intelligence, solving jigsaw puzzles [14, 31] has been widely studied for a variety of tasks in image editing [46, 10], relic re-composition [39, 3], unsupervised visual representation learning [45, 12, 37] and generalized network learning [4]. In this work, we employ Jigsaw Puzzle classifiers to learn contextual visual features (from labeled data) which are very suitable in semantic image segmentation. The learnt features are then exploited to align unlabeled target data for domain adaptive semantic segmentation.

### 3. Method

This section presents our proposed Semi-Supervised Domain Adaptive Segmentation (SSDAS) method. It consists of four subsections that focus on *Task Definition*, *Adaptive Cross-Domain Alignment (ACDA)* that performs adaptive inter-domain alignment according to the similarity of the learned features, *Progressive Intra-Domain Alignment (PIDA)* that replaces target-unlike source features by high-confidence target features for alignment between confident and unconfident target features, and *Network Training*.

#### 3.1. Preliminaries

**Task Definition:** We focus on the problem of semi-supervised domain adaptation (SSDA) in semantic segmentation. Given the labeled source images  $\{X_s \in \mathbb{R}^{H \times W \times 3}, Y_s \in (1, C)^{H \times W}\}$ , a few labeled target images  $\{X_t \in \mathbb{R}^{H \times W \times 3}, Y_t \in (1, C)^{H \times W}\}$  and a large number of unlabeled target images  $X_{t^u} \in \mathbb{R}^{H \times W \times 3}$  ( $H$ ,  $W$  and  $C$  stands for image height, image width, and the number of semantic classes, respectively), the goal of SSDA-based semantic segmentation is to learn a model  $G$  that performs well on unlabeled target-domain data  $X_{t^u}$ .

Under such data setup, a ‘S+T’ model without any domain adaptation can be derived by training over the labeled source and target images in a fully supervised manner:

$$\mathcal{L}_{s+t}(X_s, Y_s, X_t, Y_t; G) = l(G(X_s), Y_s) + l(G(X_t), Y_t), \quad (1)$$

where  $l$  denotes the standard cross entropy loss.

**Context Features Learning.** Inspired by [37, 4], we employ Jigsaw Puzzle classifier  $\mathcal{J}$  to learn context features by solving jigsaw puzzles on the predicted segmentation map  $P = G(X)$ :

$$\mathcal{L}_{jig}(P; G, \mathcal{J}) = l(\mathcal{J}(S(P, I)), I), \quad (2)$$

where ‘S’ stands for a function that decomposes the input image into  $n \times n$  patches, and shuffles and re-assigns each patch to one of the  $n^2$  grid positions (Index  $I$  records the original location index of every patch).  $\mathcal{J}$  solves jigsaw puzzle (*i.e.*, restoring the shuffled patches) by predicting the original location index (*i.e.*,  $I$ ) of patches.

Note context alignment is a simple yet efficient approach in UDA-based semantic segmentation [47, 51, 35, 48, 26]. For example, [47, 51, 35] employ adversarial learning [15] to align context features at an image level. [48, 26] first sample and cluster patches on labeled data to discover regional context features and then conduct adversarial learning to align the regional context features at a region level. Different from the aforementioned methods, our Jigsaw Puzzle method works at both region and image levels and it learns different types of context features by adjusting the jigsaw puzzle sizes and locations. Please refer to A.5. in supplementary material for more details.

#### 3.2. Adaptive Cross-Domain Alignment

This subsection describes adaptive cross-domain alignment (ACDA) that employs a few labeled target samples as references to re-weight the **features** of source samples. The features of unlabeled target samples will be aligned to the re-weighted source features for cross-domain alignment.

**Labeled Data Flow:** For labeled source images  $\{X_s, Y_s\}$  and labeled target images  $\{X_t, Y_t\}$ , we first feed them into a segmentation model  $G$  to acquire segmentation maps  $P_s = G(X_s) \in \mathbb{R}^{H \times W \times C}$  and  $P_t = G(X_t) \in \mathbb{R}^{H \times W \times C}$ . We then employ two Jigsaw Puzzle classifiers (*i.e.*,  $\mathcal{J}_s$  and  $\mathcal{J}_t$ ) to learn context features by solving jigsaw puzzles on the predicted segmentation maps:

$$\min_{G, \mathcal{J}_s, \mathcal{J}_t} \lambda_j (\mathcal{L}_{jig}(P_s; G, \mathcal{J}_s) \mathcal{M}_{cds} + \mathcal{L}_{jig}(P_t; G, \mathcal{J}_t)), \quad (3)$$

where  $\mathcal{M}_{cds} = 1 - \mathcal{N}(|\mathcal{J}_s(S(P_s, I)) - \mathcal{J}_t(S(P_s, I))|)$  is the cross-domain similarity (CDS) map that is computed based on the prediction discrepancy between the source and target Jigsaw Puzzle classifiers. It will be used to re-weight the learning loss of the source context features.  $S$  is defined in Eq. 2 and  $\mathcal{N}(x)$  is an unity-based normalization function that brings all values into the range  $[0, 1]$ . As illustrated in Fig. 1, the multiplication with  $\mathcal{M}_{cds}$  corresponds to Step A for source feature re-weighting, and the optimization of this equation corresponds to Step B for feature center updating.

**Unlabeled Data Flow:** For unlabeled target images  $X_{t^u}$ , we fix the learnt Jigsaw Puzzle classifier  $\mathcal{J}_s$  while updating the segmentation model  $G$  to solve jigsaw puzzles on the predicted segmentation maps  $P_{t^u} = G(X_{t^u})$ . This will enforce the segmentation maps  $P_{t^u}$  to have source-alike context features:

$$\min_G \lambda_j (\mathcal{L}_{jig}(P_{t^u}; G, \mathcal{J}_s)) \quad (4)$$

where the optimization of this equation corresponds to Step C that aligns target features to the updated feature centers as illustrated in Fig. 1.

#### 3.3. Progressive Intra-Domain Alignment

This subsection describes our progressive intra-domain alignment (PIDA) that replaces target-unlike source features by high-confidence target features iteratively in training. It leads to intra-domain alignment between confident and unconfident target context features.

**Labeled Data Flow:** Similar to Eq. 3, a binary removing mask  $\mathcal{M}_{rm}$  is employed to discard target-unlike source features continuously during the iterative training process, where the labeled target data flow remains unchanged:

$$\min_{G, \mathcal{J}_s, \mathcal{J}_t} \lambda_j (\mathcal{L}_{jig}(P_s; G, \mathcal{J}_s) \mathcal{M}_{rm} + \mathcal{L}_{jig}(P_t; G, \mathcal{J}_t)), \quad (5)$$

where  $\mathcal{M}_{rm}$  is obtained as described in Algorithm 1. As illustrated in Fig. 1, the multiplication with the binary mask

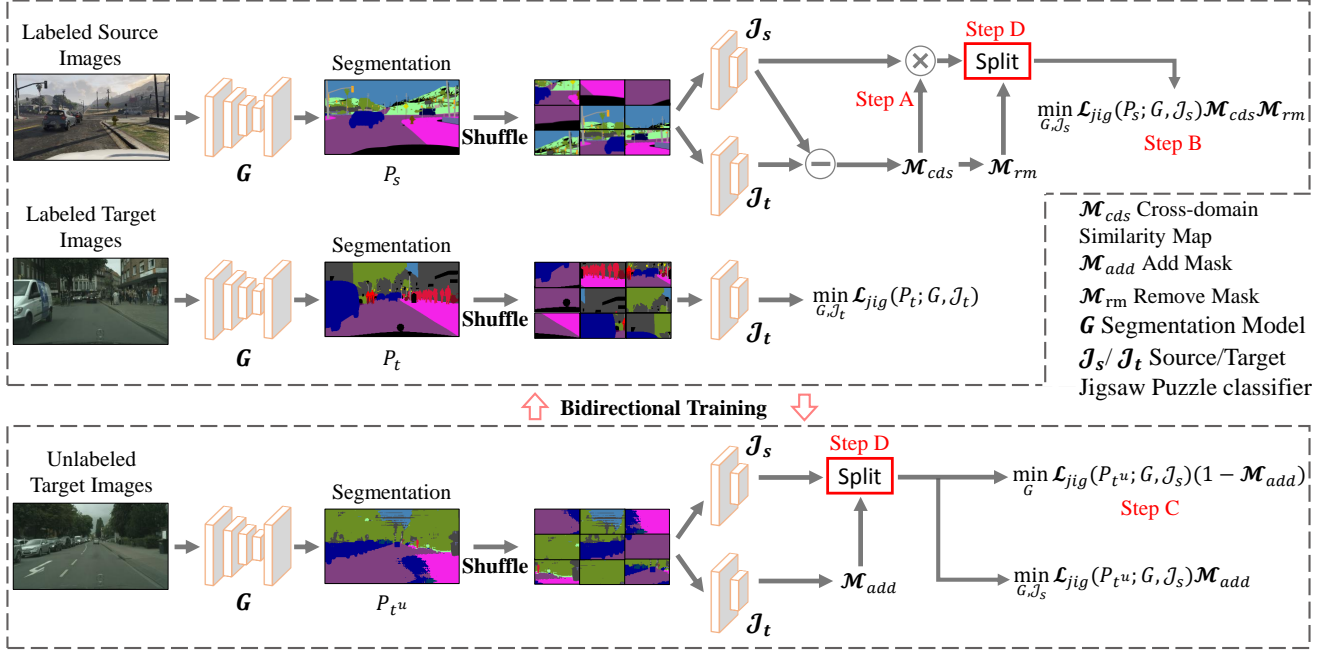


Figure 2. Overview of the proposed semi-supervised domain adaptive segmentation (SSDAS) network: SSDAS is a bidirectional training framework that consists of two alternative learning processes, namely, labeled data flow (top part) and unlabeled data flow (bottom part). In labeled data flow, we first feed the labeled source and target images (*i.e.*,  $X_s$  and  $X_t$ ) into the segmentation model  $G$  to acquire the predicted segmentation maps  $P_s$  and  $P_t$ , and then employ two Jigsaw Puzzle classifiers (*i.e.*,  $\mathcal{J}_s$  and  $\mathcal{J}_t$ ) to learning context features by solving jigsaw puzzles on  $P_s$  and  $P_t$ , respectively. In this process, Steps **A**, **B** and **D** are triggered for re-weighting each source feature, re-estimating feature centers with different treatments and removing the dissimilar source features, respectively. In unlabeled data flow (*i.e.*, for  $X_{t^u}$ ), we fix the learnt  $\mathcal{J}_s$  and update  $G$  to enforce the the segmentation maps (*i.e.*,  $P_{t^u}$ ) to have source-like context features by solving jigsaw puzzles. In this process, Steps **C** and **D** are triggered for aligning unconfident target context features to estimated feature centers and adding high-confidence target features to update  $G$  and  $\mathcal{J}_s$ , respectively.

$\mathcal{M}_{rm}$  corresponds to the Step **D** (for removing target-unlike source features), and the optimization of this equation correspond to the Step **B**.

**Unlabeled Data Flow:** Based on Eq. 4, a binary add mask  $\mathcal{M}_{add}$  is employed to inject high-confidence target features progressively for updating  $G$  and  $\mathcal{J}_s$ , where the unconfident target features will be aligned to confident target features by fixing  $\mathcal{J}_s$  while updating  $G$  during training:

$$\begin{aligned} & \min_{G, \mathcal{J}_s} \lambda_j \mathcal{L}_{jig}(P_{t^u}; G, \mathcal{J}_s) \mathcal{M}_{add}, \\ & \min_G \lambda_j \mathcal{L}_{jig}(P_{t^u}; G, \mathcal{J}_s) (1 - \mathcal{M}_{add}), \end{aligned} \quad (6)$$

where  $\mathcal{M}_{add}$  is obtained as described in Algorithm 2. As illustrated in Fig. 1, the multiplication with the binary mask  $\mathcal{M}_{add}$  corresponds to the Step **D** (injecting high-confidence target features), and the optimization of the first and second equations refer to Step **B** and Step **C**, respectively.

### 3.4. Network Training

With ACDA and PIDA as described in Sections 3.3 and 3.4, this subsection presents how ACDA and PIDA work together to achieve our proposed SSDAS. The *labeled data*

---

#### Algorithm 1 Determination of $\mathcal{M}_{rm}$ in PIDA.

---

**Require:** Source images  $X_s$ ; *epoch* denotes the epoch times; segmentation model  $G$ ; jigsaw puzzle classifiers  $\mathcal{J}_s$  and  $\mathcal{J}_t$

**Ensure:**  $\mathcal{M}_{rm}$

- 1: Calculate  $\mathcal{M}_{cds}$  as in Eq. 3
  - 2:  $\mathcal{M}_{cds}^{sort} = \text{sort}(\mathcal{M}_{cds}, \text{order}=\text{ascending})$
  - 3:  $N = \text{length}(\mathcal{M}_{cds}^{sort}) \times \frac{\text{epoch}}{\text{max.epoch}}$
  - 4:  $\text{Thres} = \mathcal{M}_{cds}^{sort}[N]$
  - 5:  $\mathcal{M}_{rm}[\mathcal{M}_{cds} \geq \text{Thres}] = 1$
  - 6:  $\mathcal{M}_{rm}[\mathcal{M}_{cds} < \text{Thres}] = 0$
  - 7: **return**  $\mathcal{M}_{rm}$
- 

*flow* is optimized as follows:

$$\min_{G, \mathcal{J}_s, \mathcal{J}_t} \lambda_j (\mathcal{L}_{jig}(P_s; G, \mathcal{J}_s) \mathcal{M}_{cds} \mathcal{M}_{rm} + \mathcal{L}_{jig}(P_t; G, \mathcal{J}_t)) \quad (7)$$

The optimization function of the *unlabeled data flow* remains unchanged as defined in Eq. 6

Note all optimization functions in Eqs. 3 - 7 are generic and can be applied for both image-level and region-level

---

**Algorithm 2** Determination of  $\mathcal{M}_{add}$  in PIDA.

**Require:** Unlabeled target images  $X_{t^u}$ ;  $epoch$  denotes the epoch times; segmentation model  $G$ ; jigsaw puzzle classifier  $\mathcal{J}_t$

**Ensure:**  $\mathcal{M}_{add}$

- 1: Calculate jigsaw puzzle classification (JPC) probability  $P_{t^u}^{jig} = \mathcal{J}_t(S(G(X_{t^u}), I))$  as in Eq. 2
  - 2: Calculate JPC entropy  $Ent_{t^u}^{jig} = P_{t^u}^{jig} \log P_{t^u}^{jig}$
  - 3:  $Ent_{t^u}^{jig-sort} = \text{sort}(Ent_{t^u}^{jig}, \text{order=ascending})$
  - 4:  $N = \text{length}(Ent_{t^u}^{jig-sort}) \times \frac{epoch}{max\_epoch}$
  - 5:  $\text{Thres} = Ent_{t^u}^{jig-sort}[N]$
  - 6:  $\mathcal{M}_{add}[Ent_{t^u}^{jig} \leq \text{Thres}] = 1$
  - 7:  $\mathcal{M}_{add}[Ent_{t^u}^{jig} > \text{Thres}] = 0$
  - 8: **return**  $\mathcal{M}_{add}$
- 

---

**Algorithm 3** The proposed Semi-Supervised Domain Adaptive Segmentation (SSDAS).

**Require:** Labeled source images  $\{X_s, Y_s\}$  and target images  $\{X_t, Y_t\}$ ; unlabeled target images  $X_{t^u}$ ;  $epoch$  denotes the epoch times; segmentation model  $G$ ; jigsaw puzzle classifiers  $\mathcal{J}_s^{image}$ ,  $\mathcal{J}_t^{image}$ ,  $\mathcal{J}_s^{region}$  and  $\mathcal{J}_t^{region}$ ; region crop size  $r$

**Ensure:** Learnt parameters  $\theta$  of segmentation model  $G$

- 1: **for**  $epoch = 1$  **to**  $max\_epoch$  **do**
  - 2: **Supervised segmentation learning:**
  - 3: Update  $G$  using Eq. 1 with  $\{X_s, Y_s\}$  and  $\{X_t, Y_t\}$
  - 4: **Image-level alignment:** ACDA&PIDA
  - 5: Calculate segmentation probability map  $P_s = G(X_s)$ ,  $P_t = G(X_t)$  and  $P_{t^u} = G(X_{t^u})$
  - 6: Update  $G$ ,  $\mathcal{J}_s^{image}$  and  $\mathcal{J}_t^{image}$  using Eq. 7 and Eq. 6 with  $P_s$ ,  $P_t$  and  $P_{t^u}$
  - 7: **Region-level alignment:** ACDA&PIDA
  - 8: Crop maps into  $r \times r$  regions  $P_s^{region} = \{P_s^0, P_s^1, \dots, P_s^{r^2}\}$ ,  $P_t^{region} = \{P_t^0, P_t^1, \dots, P_t^{r^2}\}$  and  $P_{t^u}^{region} = \{P_{t^u}^0, P_{t^u}^1, \dots, P_{t^u}^{r^2}\}$
  - 9: Update  $G$ ,  $\mathcal{J}_s^{region}$  and  $\mathcal{J}_t^{region}$  using Eq. 7 and Eq. 6 with  $P_s^{region}$ ,  $P_t^{region}$  and  $P_{t^u}^{region}$
  - 10: **end for**
  - 11: **return**  $G$
- 

alignments. The only difference lies with the input. Specifically, the image-level alignment takes a whole segmentation map as input. But for *region-level alignment*, the segmentation map  $P$  (i.e.,  $P_s$ ,  $P_t$  and  $P_{t^u}$ ) is cropped into  $r \times r$  regions which are fed into the extra region-level Jigsaw Puzzle Classifiers ( $\mathcal{J}_s^{region}$  and  $\mathcal{J}_t^{region}$ ) for regional context features learning and alignment. The entire training pipeline is summarized in Algorithm. 3.

Image-level Alignment		Region-level Alignment		mIoU
ACDA	PIDA	ACDA	PIDA	
				37.9
✓				43.6
	✓			41.7
✓	✓			45.1
		✓		44.8
			✓	41.9
		✓	✓	46.2
✓		✓		46.3
	✓		✓	44.5
✓	✓	✓	✓	<b>48.5</b>

Table 1. Ablation study of SSDAS over semi-supervised domain adaptive segmentation task GTA  $\rightarrow$  Cityscapes. The 1st row shows ‘‘S+T’’ model that is trained with supervised segmentation loss with labeled source and target samples only (without any alignment) as defined in Eq. 1. The backbone is ResNet-101 and the setting is one-shot as evaluated in mIoU.

## 4. Experiments

This section presents the evaluation of our SSDAS including datasets and implementation details, comparisons with the state-of-the-art, ablation studies, and discussion, more details to be described in the ensuing subsections.

### 4.1. Experiment Setups

In our experiments, we followed the setting of [40] that focuses on SSDA-based image classification. The training data consist of three parts including labeled source samples, unlabeled target samples, and 1 or 3 labeled target samples that are randomly selected for 1-shot or 3-shot SSDA-based semantic segmentation, respectively.

**Datasets:** We evaluated SSDAS over two challenging domain adaptive segmentation tasks GTA5 $\rightarrow$ Cityscapes and SYNTHIA $\rightarrow$ Cityscapes, which involve two synthetic source datasets and one real target dataset. Specifically, Cityscapes consists of 2975 training images and 500 validation images. GTA5 and SYNTHIA consist of 24,966 and 9,400 high-resolution synthetic images which share 19 and 16 classes with Cityscapes. We also evaluated SSDAS on domain adaptive classification over the dataset Office-Home [50] that has 65 image classes of 4 domains.

**Implementation Details.** All our experiments were implemented in Pytorch. The segmentation model  $G$  uses ResNet101 [19] (pre-trained with ImageNet [11]) with DeepLab-V2 [5]. The optimizer is SGD [2] with a momentum of 0.9 and a weight decay of  $1e-4$ . The learning rate is  $2.5e-4$  initially and decreased by a polynomial policy with a power of 0.9. Except parameter studies in Table 7, we set the trade-off parameter  $\lambda_j$  at 0.1 and the number of Jigsaw Puzzle classes  $N$  at 100 in all other experiments. The Jigsaw Puzzle classifiers (i.e.,  $\mathcal{J}_s$  and  $\mathcal{J}_t$ ) are pre-trained with

Setting	Method	Road	SW	Build	Wall	Fence	Pole	TL	TS	Veg.	Terrain	Sky	PR	Rider	Car	Truck	Bus	Train	Motor	Bike	mIoU
1-shot	S+T	82.1	22.8	72.8	20.3	22.0	26.7	31.1	11.8	75.7	24.0	76.8	56.2	23.2	71.4	21.6	20.7	0.1	28.5	32.5	37.9
	AdaptSeg [47]	87.0	32.8	80.5	22.1	22.6	27.7	34.3	25.4	83.4	31.5	81.7	59.5	18.6	76.0	35.4	42.9	1.6	28.0	27.1	43.1
	ADVENT [51]	92.3	52.8	81.9	30.0	25.6	28.8	35.4	24.0	84.9	39.1	79.4	56.1	21.4	86.3	31.1	33.5	1.2	30.8	11.1	44.5
	CRST [58]	91.5	51.7	81.6	28.3	<b>28.5</b>	<b>43.9</b>	45.0	26.7	85.2	35.4	65.0	<b>68.8</b>	29.2	85.5	32.8	28.4	1.3	31.0	<b>42.0</b>	47.5
	FDA [52]	90.5	40.9	80.2	26.0	25.0	31.1	32.6	34.5	80.3	33.7	79.5	54.0	30.2	83.8	35.0	41.2	11.8	21.1	30.7	45.4
	IDA [38]	92.7	53.2	82.9	31.9	19.7	29.9	35.6	22.5	86.2	45.8	<b>82.4</b>	57.8	26.6	87.9	33.2	42.7	1.1	<b>32.9</b>	24.3	46.8
	SSDAS	92.9	53.9	82.1	31.5	24.0	36.4	40.6	33.8	84.5	44.9	69.6	60.5	25.4	85.1	<b>46.9</b>	52.4	2.7	19.2	34.3	48.5
	+ADVENT	93.2	54.1	82.4	32.8	25.4	34.0	39.5	36.7	85.0	45.7	80.4	60.7	26.8	84.3	42.5	<b>52.5</b>	3.1	28.5	29.4	49.3
	+CRST	<b>94.1</b>	60.8	<b>83.9</b>	<b>35.3</b>	17.5	40.1	<b>50.6</b>	<b>47.1</b>	85.2	45.6	81.2	66.3	26.9	<b>88.6</b>	33.7	49.1	10.7	22.7	35.8	<b>51.3</b>
	+FDA	93.9	52.0	83.3	28.2	26.8	38.9	37.6	38.6	<b>82.7</b>	40.7	81.4	54.4	<b>32.9</b>	86.6	42.1	49.3	<b>14.8</b>	22.8	34.9	49.6
+IDA	93.7	<b>56.7</b>	83.8	33.9	25.7	35.8	40.3	38.2	<b>86.6</b>	<b>46.1</b>	81.2	60.0	25.1	87.8	34.1	47.1	3.3	26.1	34.8	49.5	
3-shot	S+T	73.2	29.9	75.4	17.6	20.4	30.5	34.7	24.5	80.8	26.0	76.0	58.1	28.1	45.1	34.8	34.1	0.6	26.9	37.0	39.7
	AdaptSeg [47]	86.6	43.3	80.7	22.1	21.9	26.1	33.4	27.0	82.8	28.8	80.6	58.1	26.1	77.9	37.2	42.0	1.1	24.8	29.6	43.7
	ADVENT [51]	92.3	51.1	81.8	29.7	23.7	31.9	32.7	18.2	84.4	35.5	75.6	57.8	21.5	86.7	35.3	48.0	0.7	28.4	19.7	45.0
	CRST [58]	92.2	52.1	81.6	24.7	27.5	41.0	<b>45.8</b>	27.6	83.6	34.2	76.4	63.6	22.4	86.3	33.1	48.0	5.9	28.3	38.2	48.0
	FDA [52]	91.6	45.5	82.4	25.8	25.5	30.7	34.2	30.2	82.7	29.2	79.9	60.3	28.1	87.0	33.2	37.4	8.8	22.6	34.8	45.8
	IDA [38]	92.6	52.2	83.3	30.3	26.7	33.0	35.7	25.2	85.2	42.9	79.5	59.2	27.0	87.3	37.0	48.9	4.5	30.2	12.5	47.0
	SSDAS	92.4	52.6	83.7	27.0	20.9	37.5	41.5	36.3	85.3	42.2	78.7	63.1	32.0	86.8	45.7	49.6	5.9	20.2	42.3	49.7
	+ADVENT	<b>93.9</b>	52.0	83.3	29.2	26.8	38.9	40.6	38.6	<b>85.7</b>	41.7	81.4	59.4	32.9	86.6	42.1	49.3	<b>14.8</b>	22.8	34.9	50.3
	+CRST	93.6	<b>58.1</b>	83.5	<b>32.1</b>	<b>28.1</b>	<b>42.7</b>	43.8	<b>41.4</b>	85.5	42.1	81.8	<b>64.9</b>	<b>33.7</b>	<b>87.9</b>	<b>46.8</b>	<b>49.5</b>	13.5	<b>31.9</b>	43.3	<b>52.9</b>
	+FDA	93.3	49.8	83.1	31.3	25.7	37.2	39.1	38.0	85.6	<b>43.2</b>	81.4	61.9	30.1	86.4	43.9	<b>50.3</b>	9.4	25.6	<b>43.9</b>	50.5
+IDA	93.6	56.3	<b>84.3</b>	25.3	21.6	38.2	41.6	38.7	85.6	40.0	<b>82.5</b>	61.6	29.4	86.0	42.2	48.6	7.6	29.9	42.6	50.3	

Table 2. Comparing SSDAS with state-of-the-art semantic segmentation methods: For semi-supervised domain adaptive semantic segmentation task GTA  $\rightarrow$  Cityscapes, the proposed SSDAS consistently outperforms all state-of-the-art UDA methods that are adapted for the SSDA task. In addition, SSDAS is clearly complementary to all adapted UDA methods with clear performance gains. The backbone is ResNet-101 for all compared methods, and the setting includes 1-shot and 3-shot.

Setting	Method	Road	SW	Build	Wall*	Fence*	Pole*	TL	TS	Veg.	Sky	PR	Rider	Car	Bus	Motor	Bike	mIoU	mIoU*
1-shot	S+T	56.3	17.6	76.3	9.9	2.1	28.3	14.3	13.8	80.0	80.9	51.2	14.2	43.1	22.1	19.0	24.6	34.6	39.5
	AdaptSeg [47]	84.2	41.4	78.0	10.1	0.5	27.8	6.1	11.7	81.8	79.5	54.3	21.9	70.8	35.3	12.3	32.8	40.5	46.9
	ADVENT [51]	87.2	45.3	78.7	9.2	2.8	23.6	6.7	14.7	80.9	83.3	58.8	22.0	71.3	31.4	10.8	35.1	41.4	48.2
	CRST [58]	69.9	31.8	74.9	14.8	3.6	37.0	22.5	29.5	81.6	79.1	58.2	28.8	83.6	27.2	22.9	46.6	44.5	50.5
	FDA [52]	78.2	32.5	73.0	11.2	2.4	27.8	16.1	17.5	80.0	82.0	52.5	24.7	74.3	34.3	20.0	39.8	41.6	48.1
	IDA [38]	84.7	38.3	78.8	10.5	2.9	27.0	13.6	12.3	80.5	<b>83.8</b>	57.7	22.9	72.0	38.0	20.7	35.8	42.5	49.2
	SSDAS	87.6	44.4	79.1	13.2	3.2	29.8	14.1	18.4	81.0	80.8	58.0	26.3	77.3	39.7	19.4	38.6	44.4	51.1
	+ADVENT	<b>88.6</b>	<b>46.2</b>	78.8	14.1	2.2	28.9	16.8	21.5	80.9	82.5	58.9	25.5	78.7	37.5	20.3	41.9	45.2	52.2
	+CRST	86.8	45.7	79.4	<b>15.2</b>	3.1	<b>39.7</b>	<b>24.0</b>	<b>31.9</b>	<b>82.5</b>	79.6	57.7	<b>29.1</b>	<b>84.4</b>	<b>41.5</b>	<b>25.2</b>	<b>48.7</b>	<b>48.4</b>	<b>55.1</b>
	+FDA	86.3	43.6	78.1	14.5	<b>4.1</b>	32.3	18.6	20.0	80.1	82.8	57.4	27.9	79.8	40.1	22.8	43.9	45.8	52.4
+IDA	87.3	44.9	<b>80.2</b>	12.2	2.1	30.8	12.3	21.3	81.8	83.7	<b>59.4</b>	27.1	75.4	40.9	21.8	41.9	45.2	52.2	
3-shot	S+T	58.4	24.3	77.3	9.8	2.4	27.4	12.6	16.1	77.7	78.7	51.6	18.7	40.0	28.7	17.0	30.3	35.7	40.9
	AdaptSeg [47]	84.7	38.9	78.1	12.6	2.1	28.2	8.8	12.3	80.9	80.1	55.4	19.5	72.7	35.6	14.6	32.2	41.0	47.2
	ADVENT [51]	86.8	44.3	79.2	14.1	4.1	28.6	13.2	18.8	81.4	82.7	56.7	21.0	77.2	33.1	12.6	27.1	42.6	48.8
	CRST [58]	72.6	36.3	76.9	15.2	4.1	37.5	21.1	28.6	81.9	82.5	57.8	27.4	82.4	30.5	20.1	42.2	44.8	50.8
	FDA [52]	81.6	36.6	74.2	15.6	3.1	26.5	18.1	19.9	82.3	83.0	55.2	18.6	80.7	27.5	19.9	34.5	42.3	48.6
	IDA [38]	85.5	40.0	78.6	14.2	3.1	25.3	16.3	18.3	80.5	82.2	54.9	19.4	75.9	39.6	19.8	32.5	42.9	49.5
	SSDAS	88.5	45.1	78.2	15.0	3.0	29.2	19.9	21.3	80.8	82.6	58.5	26.0	76.0	37.9	21.4	40.0	45.2	52.0
	+ADVENT	88.7	46.6	79.9	16.9	4.1	32.6	20.2	20.3	81.9	83.5	57.5	26.4	80.7	38.1	22.3	38.7	46.2	52.7
	+CRST	<b>89.1</b>	<b>46.7</b>	<b>80.2</b>	16.6	4.2	<b>40.5</b>	<b>23.8</b>	<b>32.9</b>	82.8	<b>83.5</b>	<b>59.7</b>	<b>29.3</b>	<b>84.6</b>	<b>41.0</b>	<b>24.1</b>	<b>47.3</b>	<b>49.1</b>	<b>55.8</b>
	+FDA	88.0	43.7	78.0	<b>17.6</b>	<b>5.2</b>	31.8	22.9	20.4	<b>83.4</b>	<b>83.8</b>	56.2	27.7	81.0	38.1	22.6	42.9	46.5	53.0
+IDA	87.9	46.3	79.4	16.4	4.0	30.7	22.0	20.1	82.6	83.1	57.3	27.9	80.8	40.2	20.4	38.9	46.1	52.8	

Table 3. Comparing SSDAS with state-of-the-art semantic segmentation methods: For semi-supervised domain adaptive semantic segmentation task SYNTHIA  $\rightarrow$  Cityscapes, the proposed SSDAS consistently outperforms all state-of-the-art UDA methods that are adapted for the SSDA task. In addition, SSDAS is clearly complementary to all adapted UDA methods with clear performance gains. The backbone is ResNet-101 for all compared methods, and the setting includes 1-shot and 3-shot.

“S+T” model to avoid noisy predictions at the initial training stage. We freeze Jigsaw Puzzle classifier  $\mathcal{J}_t$  when its training loss is smaller than  $\mathcal{J}_s$ 's to avoid over-fitting with just a few labeled target samples. For SSDA-based classification, we follow the setting in [40].

## 4.2. Ablation Studies

We first examine different SSDAS components to study their contributions to SSDA-based semantic segmentation. Table 1 shows experimental results over the validation set of

Cityscapes, where the first row shows the result of “S+T” model that is trained with supervised loss with labeled source and target samples only (with no alignment) as defined in Eq. 1. It can be seen that “S+T” model does not perform well due to cross-domain gaps.

However, ACDA improves “S+T” model clearly at both region and image levels, largely because ACDA employs few-shot target features to re-weight source features adaptively by increasing (or decreasing) the weight of target-alike (or target-unlike) source features. Further including

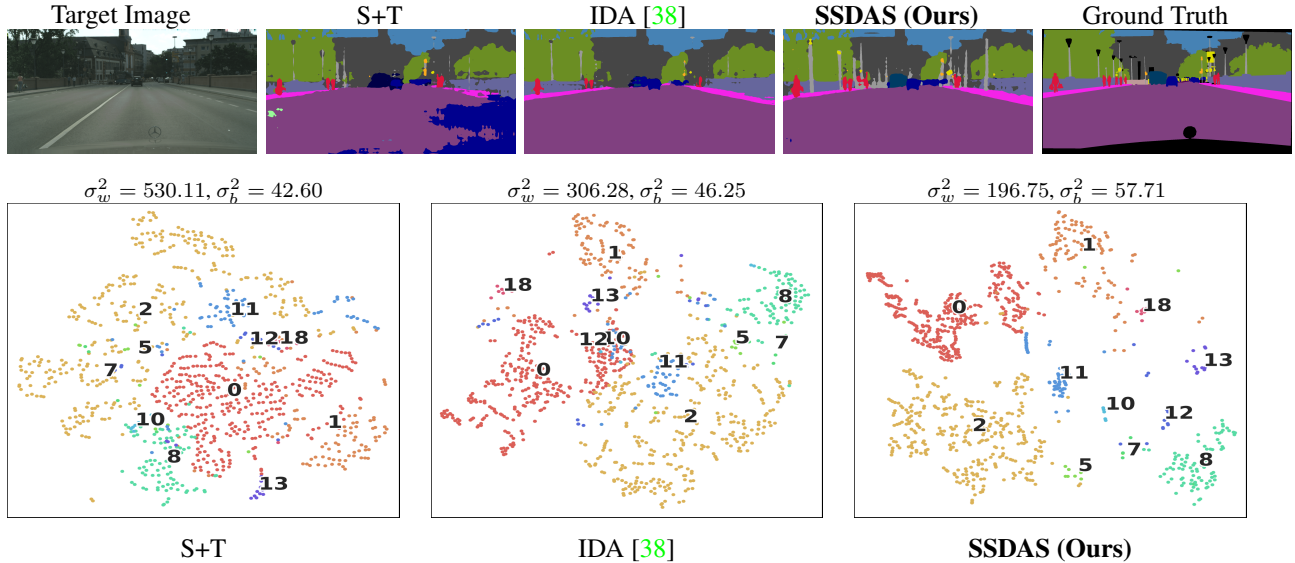


Figure 3. **First row:** Qualitative illustration of semi-supervised domain adaptive semantic segmentation for GTA5  $\rightarrow$  Cityscapes adaptation. SSDAS employs a few labeled target sample as anchors for adaptive and progressive feature alignment between labeled source samples and unlabeled target samples, which produces nice semantic segmentation especially for the challenging low-frequency categories such as pole, bus and traffic-light etc. **Second row:** t-SNE [36] visualization of feature distribution for target images in task GTA  $\rightarrow$  Cityscapes: Each colour represents one semantic class of image pixels with a digit showing the class centre.  $\sigma_w^2$  and  $\sigma_b^2$  on the top of each graph are intra-class variance and inter-class distance of the corresponding feature distribution. The proposed SSDAS greatly outperforms “S+T” and “IDA” baselines in domain adaptive semantic segmentation qualitatively and quantitatively.

Network	Method	GTA $\rightarrow$ City	
		1-shot	3-shot
ResNet-101	S+T	37.9	39.7
	ENT [16]	42.8	43.5
	MME [40]	43.2	43.8
	<b>SSDAS</b>	<b>48.5</b>	<b>49.7</b>

Table 4. Comparing our SSDAS with state-of-the-art SSDA classification methods (in mIoU): For domain adaptive semantic segmentation task GTA  $\rightarrow$  Cityscapes, SSDAS outperforms the state-of-the-art by large margins consistently for both 1-shot and 3-shot.

PIDA improves mIoU by another +1.4% at both image and region levels, demonstrating its effectiveness in intra-domain alignment. It also shows that ACDA and PIDA are complementary by focusing on cross-domain alignment and intra-domain alignment, respectively.

The last three rows show that including image-level alignment and region-level alignment simultaneously outperforms adopting either one alone for both ACDA and PIDA. This shows that our proposed image-level and region-level alignment are complementary, where the image-level alignment focuses more on classes with big sizes (*e.g.*, road, building, sky, etc.) while the region-level alignment focuses more on classes with small sizes (*e.g.*, person, car, bike, etc.). Finally, including both alignment strategies at both image and region levels (*i.e.*, the complete SSDAS model) performs clearly the best.

### 4.3. Comparisons with the State-of-Art

As there is few prior work on SSDA-based semantic segmentation, we conducted two sets of experiments to benchmark our SSDAS with the state-of-the-art. In the first set of experiments, we adapted state-of-the-art UDA methods for the SSDA task. Specifically, we included the labeled target samples and the corresponding supervised loss into the UDA methods to approximate SSDA-based semantic segmentation. Tables 2 and 3 show representative UDA methods (‘AdaptSeg’, ‘ADVENT’, ‘CRST’, ‘FDA’ and ‘CrCDA’) and their results. It can be seen that our SSDAS outperforms all adapted UDA methods consistently for both tasks GTA5 $\rightarrow$ Cityscapes and SYNTHIA $\rightarrow$ Cityscapes. The superior segmentation is largely attributed to the adaptive and progressive feature alignment in SSDAS that exploits the few-shot labeled target samples to guide the cross-domain and intra-domain alignment effectively.

In the second set of experiments, we benchmarked SSDAS with state-of-the-art SSDA-based image classification methods for both semantic segmentation and image classification tasks. To adapt SSDAS for image classification, we simply take the feature maps instead of segmentation maps as the Jigsaw Puzzle input with little fine-tuning. Tables 4 and 5 show experimental results. For the semantic segmentation in Table 4, we can see that SSDAS outperforms SSDA classification methods by large margins (over 5.3% in mIoU) for both 1-shot and 3-shot settings. For the image

Network	Method	R to C	R to P	R to A	P to R	P to C	P to A	A to P	A to C	A to R	C to R	C to A	C to P	MEAN
ResNet-34	S+T	55.7	80.8	67.8	73.1	53.8	63.5	73.1	54.0	74.2	68.3	57.6	72.3	66.2
	ENT [16]	62.6	85.7	70.2	79.9	60.5	63.9	79.5	61.3	79.1	76.4	64.7	79.1	71.9
	MME [40]	64.6	85.5	71.3	80.1	64.6	65.5	79.0	63.6	79.7	76.6	<b>67.2</b>	79.3	73.1
	APE [30]	66.4	86.2	73.4	82.0	65.2	66.1	81.1	<b>63.9</b>	80.2	76.8	66.6	79.9	74.0
	<b>SSDAS</b>	<b>69.1</b>	<b>86.9</b>	<b>76.2</b>	<b>83.4</b>	<b>66.8</b>	<b>67.5</b>	<b>83.5</b>	63.8	<b>82.3</b>	<b>77.9</b>	67.0	<b>81.1</b>	<b>75.5</b>

Table 5. Comparing SSDAS with state-of-the-art SSDA classification methods: For domain adaptive image classification task (3-shot), the proposed SSDAS outperforms the state-of-the-art clearly in most of 12 adaptation scenarios in Office-home dataset.

The number of the labeled target samples					
Method	1	3	5	10	20
S+T	37.9	39.7	40.4	41.7	44.6
<b>SSDAS</b>	<b>48.5</b>	<b>49.7</b>	<b>50.1</b>	<b>51.1</b>	<b>52.6</b>

Table 6. The number of labeled target samples matters: Domain adaptive semantic segmentation keeps improving with the increase of labeled target samples (over the task GTA → Cityscapes).

Parameter Analysis of $\lambda_j$ and $N$					
$\lambda_j$	0.025	0.05	0.1	0.2	0.4
SSDAS	47.9	48.3	48.5	48.4	48.1
$N$	30	50	100	300	500
SSDAS	48.2	48.3	48.5	48.4	48.4

Table 7. The weight parameter  $\lambda_j$  and the number of Jigsaw Puzzle classes  $N$  matter: Domain adaptive semantic segmentation is slightly affected by  $\lambda_j$  but tolerant to  $N$  (for GTA → Cityscapes).

Method	Convention-feature	Context-feature	mIoU
SSDAS	✓		47.1
		✓	48.5
	✓	✓	49.7

Table 8. SSDAS is generic and can work for other features such as conventional features. For the task GTA → Cityscapes, we employ SSDAS to aligning the convention-feature and context-feature, and present the domain adaptive semantic segmentation performance in mIoU.

classification task in Table 5, SSDAS outperforms state-of-the-art SSDA classification methods clearly as well. These experiments show that SSDAS is generic for different tasks.

#### 4.4. Discussion

**Number of labeled target samples:** We studied how SSDAS behaves while including more labeled target samples in training. The experiments in Table 6 shows that domain adaptive segmentation can be improved consistently when more labeled target samples are included.

**The weight  $\lambda_j$  and the number of Jigsaw Puzzle classes  $N$ :** Parameters  $\lambda_j$  and  $N$  control the weights of supervised and unsupervised losses and the difficulty of Jigsaw Puzzle, respectively. We studied the two parameters by changing  $\lambda_j$  from 0 to 1 with a step of 1/6 and setting  $N$  at a few number as shown in Table 7. Experiments over the task

GTA→Cityscapes show that SSDAS is tolerant to both  $\lambda_j$  and  $N$ . The major reason is that the adaptive and progressive learning in SSDAS can alleviate ‘negative alignment’ with dissimilar features.

**Context vs conventional features:** We use context feature in this work but SSDAS can also work with conventional segmentation features, i.e. the features from the feature extractor  $E$  without including the following Jigsaw Puzzle classifiers. To work with conventional features, the algorithm and optimization functions are the same (as with context features) except that the context features are replaced by conventional features. Please refer to Section A.1. of supplementary materials for details about the optimization functions and algorithms of aligning conventional features. Table 8 compares SSDAS while working with context and conventional features. We can observe that SSDAS can work with convention features well though the segmentation performance drops clearly. The performance drop is largely due to the fact that context features capture context information and are more effective in semantic segmentation. In addition, experiments show that context and conventional features are complementary while working together in domain adaptive semantic segmentation.

Moreover, we provide qualitative comparison and feature distribution visualization over the task GTA5→Cityscapes in Fig. 3. Due to the space limit, more discussion and qualitative comparisons over domain adaptive segmentation task are provided in the appendix.

## 5. Conclusion

In this work, we presented SSDAS, a Semi-Supervised Domain Adaptive image Segmentation network that employs a few labeled target samples as anchors for adaptive and progressive feature alignment between labeled source samples and unlabeled target samples. To the best of our knowledge, this is the first effort towards semi-supervised domain adaptive semantic segmentation (with few-shot target samples). Extensive experiments demonstrate the superiority of our SSDAS over a number of baselines including UDA-based segmentation and SSDA-based classification methods. In addition, SSDAS is complementary and can be easily integrated with UDA-based methods with consistent improvements in segmentation. We will explore how to bet-



ter make use of a few labeled target samples in SSDA-based semantic segmentation. In addition, we will also study how to extend the idea of our SSDAS to other computer vision tasks such as object detection and panoptic segmentation.

## Acknowledgement

This research was conducted in collaboration with Singapore Telecommunications Limited and supported/partially supported (delete as appropriate) by the Singapore Government through the Industry Alignment Fund - Industry Collaboration Projects Grant.

## References

- [1] Shuang Ao, Xiang Li, and Charles Ling. Fast generalized distillation for semi-supervised domain adaptation. In *Proceedings of the AAAI Conference on Artificial Intelligence*, volume 31, 2017. 2
- [2] Léon Bottou. Large-scale machine learning with stochastic gradient descent. In *Proceedings of COMPSTAT'2010*, pages 177–186. Springer, 2010. 5
- [3] Benedict J Brown, Corey Toler-Franklin, Diego Nehab, Michael Burns, David Dobkin, Andreas Vlachopoulos, Christos Doumas, Szymon Rusinkiewicz, and Tim Weyrich. A system for high-volume acquisition and matching of fresco fragments: Reassembling theran wall paintings. *ACM transactions on graphics (TOG)*, 27(3):1–9, 2008. 2
- [4] Fabio M Carlucci, Antonio D’Innocente, Silvia Bucci, Barbara Caputo, and Tatiana Tommasi. Domain generalization by solving jigsaw puzzles. In *Proceedings of the IEEE/CVF Conference on Computer Vision and Pattern Recognition*, pages 2229–2238, 2019. 2, 3
- [5] Liang-Chieh Chen, George Papandreou, Iasonas Kokkinos, Kevin Murphy, and Alan L Yuille. Deeplab: Semantic image segmentation with deep convolutional nets, atrous convolution, and fully connected crfs. *IEEE transactions on pattern analysis and machine intelligence*, 40(4):834–848, 2017. 5
- [6] Qingchao Chen, Yang Liu, Zhaowen Wang, Ian Wassell, and Kevin Chetty. Re-weighted adversarial adaptation network for unsupervised domain adaptation. In *The IEEE Conference on Computer Vision and Pattern Recognition (CVPR)*, June 2018. 1
- [7] Yuhua Chen, Wen Li, Christos Sakaridis, Dengxin Dai, and Luc Van Gool. Domain adaptive faster r-cnn for object detection in the wild. In *Proceedings of the IEEE conference on computer vision and pattern recognition*, pages 3339–3348, 2018. 1
- [8] Yuhua Chen, Wen Li, and Luc Van Gool. Road: Reality oriented adaptation for semantic segmentation of urban scenes. In *Proceedings of the IEEE Conference on Computer Vision and Pattern Recognition*, pages 7892–7901, 2018. 2
- [9] Yun-Chun Chen, Yen-Yu Lin, Ming-Hsuan Yang, and Jia-Bin Huang. Crdoco: Pixel-level domain transfer with cross-domain consistency. In *Proceedings of the IEEE Conference on Computer Vision and Pattern Recognition*, pages 1791–1800, 2019. 2
- [10] Taeg Sang Cho, Shai Avidan, and William T Freeman. The patch transform. *IEEE transactions on pattern analysis and machine intelligence*, 32(8):1489–1501, 2009. 2
- [11] Jia Deng, Wei Dong, Richard Socher, Li-Jia Li, Kai Li, and Li Fei-Fei. Imagenet: A large-scale hierarchical image database. In *2009 IEEE conference on computer vision and pattern recognition*, pages 248–255. Ieee, 2009. 5
- [12] Carl Doersch, Abhinav Gupta, and Alexei A Efros. Unsupervised visual representation learning by context prediction. In *Proceedings of the IEEE international conference on computer vision*, pages 1422–1430, 2015. 2
- [13] Jeff Donahue, Judy Hoffman, Erik Rodner, Kate Saenko, and Trevor Darrell. Semi-supervised domain adaptation with instance constraints. In *Proceedings of the IEEE conference on computer vision and pattern recognition*, pages 668–675, 2013. 2
- [14] Herbert Freeman and L Garder. Apictorial jigsaw puzzles: The computer solution of a problem in pattern recognition. *IEEE Transactions on Electronic Computers*, (2):118–127, 1964. 2
- [15] Ian Goodfellow, Jean Pouget-Abadie, Mehdi Mirza, Bing Xu, David Warde-Farley, Sherjil Ozair, Aaron Courville, and Yoshua Bengio. Generative adversarial nets. In *Advances in neural information processing systems*, pages 2672–2680, 2014. 3
- [16] Yves Grandvalet and Yoshua Bengio. Semi-supervised learning by entropy minimization. In *Advances in neural information processing systems*, pages 529–536, 2005. 7, 8
- [17] Dayan Guan, Jiaying Huang, Shijian Lu, and Aoran Xiao. Scale variance minimization for unsupervised domain adaptation in image segmentation. *Pattern Recognition*, 112:107764, 2021. 2
- [18] Dayan Guan, Jiaying Huang, Aoran Xiao, Shijian Lu, and Yanpeng Cao. Uncertainty-aware unsupervised domain adaptation in object detection. *IEEE Transactions on Multimedia*, 2021. 2
- [19] Kaiming He, Xiangyu Zhang, Shaoqing Ren, and Jian Sun. Deep residual learning for image recognition. In *Proceedings of the IEEE conference on computer vision and pattern recognition*, pages 770–778, 2016. 5
- [20] Judy Hoffman, Eric Tzeng, Taesung Park, Jun-Yan Zhu, Phillip Isola, Kate Saenko, Alexei Efros, and Trevor Darrell. Cycada: Cycle-consistent adversarial domain adaptation. In *International Conference on Machine Learning*, pages 1989–1998, 2018. 2
- [21] Judy Hoffman, Dequan Wang, Fisher Yu, and Trevor Darrell. Fcns in the wild: Pixel-level adversarial and constraint-based adaptation. *arXiv preprint arXiv:1612.02649*, 2016. 1, 2
- [22] Weixiang Hong, Zhenzhen Wang, Ming Yang, and Junsong Yuan. Conditional generative adversarial network for structured domain adaptation. In *Proceedings of the IEEE Conference on Computer Vision and Pattern Recognition*, pages 1335–1344, 2018. 2
- [23] Jiaying Huang, Dayan Guan, Shijian Lu, and Aoran Xiao. Mlan: Multi-level adversarial network for domain adaptive semantic segmentation. *arXiv preprint arXiv:2103.12991*, 2021. 2

- [24] Jiaxing Huang, Dayan Guan, Aoran Xiao, and Shijian Lu. Cross-view regularization for domain adaptive panoptic segmentation. *arXiv preprint arXiv:2103.02584*, 2021. [2](#)
- [25] Jiaxing Huang, Dayan Guan, Aoran Xiao, and Shijian Lu. Fskr: Frequency space domain randomization for domain generalization. *arXiv preprint arXiv:2103.02370*, 2021. [2](#)
- [26] Jiaxing Huang, Shijian Lu, Dayan Guan, and Xiaobing Zhang. Contextual-relation consistent domain adaptation for semantic segmentation. In *European Conference on Computer Vision*, pages 705–722. Springer, 2020. [3](#)
- [27] Pin Jiang, Aming Wu, Yahong Han, Yunfeng Shao, Meiyu Qi, and Bingshuai Li. Bidirectional adversarial training for semi-supervised domain adaptation. [2](#)
- [28] Guoliang Kang, Lu Jiang, Yi Yang, and Alexander G Hauptmann. Contrastive adaptation network for unsupervised domain adaptation. In *Proceedings of the IEEE Conference on Computer Vision and Pattern Recognition*, pages 4893–4902, 2019. [1](#)
- [29] Guoliang Kang, Liang Zheng, Yan Yan, and Yi Yang. Deep adversarial attention alignment for unsupervised domain adaptation: the benefit of target expectation maximization. In *Proceedings of the European Conference on Computer Vision (ECCV)*, pages 401–416, 2018. [1](#)
- [30] Taekyung Kim and Changick Kim. Attract, perturb, and explore: Learning a feature alignment network for semi-supervised domain adaptation. In *European Conference on Computer Vision*, pages 591–607. Springer, 2020. [2](#), [8](#)
- [31] David A Kosiba, Pierre M Devaux, Sanjay Balasubramanian, Tarak L Gandhi, and K Kasturi. An automatic jigsaw puzzle solver. In *Proceedings of 12th International Conference on Pattern Recognition*, volume 1, pages 616–618. IEEE, 1994. [2](#)
- [32] Chen-Yu Lee, Tanmay Batra, Mohammad Haris Baig, and Daniel Ulbricht. Sliced wasserstein discrepancy for unsupervised domain adaptation. In *Proceedings of the IEEE Conference on Computer Vision and Pattern Recognition*, pages 10285–10295, 2019. [2](#)
- [33] Yunsheng Li, Lu Yuan, and Nuno Vasconcelos. Bidirectional learning for domain adaptation of semantic segmentation. In *Proceedings of the IEEE Conference on Computer Vision and Pattern Recognition*, pages 6936–6945, 2019. [2](#)
- [34] Mingsheng Long, Han Zhu, Jianmin Wang, and Michael I Jordan. Unsupervised domain adaptation with residual transfer networks. In *Advances in Neural Information Processing Systems*, pages 136–144, 2016. [2](#)
- [35] Yawei Luo, Liang Zheng, Tao Guan, Junqing Yu, and Yi Yang. Taking a closer look at domain shift: Category-level adversaries for semantics consistent domain adaptation. In *Proceedings of the IEEE Conference on Computer Vision and Pattern Recognition*, pages 2507–2516, 2019. [1](#), [2](#), [3](#)
- [36] Laurens van der Maaten and Geoffrey Hinton. Visualizing data using t-sne. *Journal of machine learning research*, 9(Nov):2579–2605, 2008. [7](#)
- [37] Mehdi Noroozi and Paolo Favaro. Unsupervised learning of visual representations by solving jigsaw puzzles. In *European conference on computer vision*, pages 69–84. Springer, 2016. [2](#), [3](#)
- [38] Fei Pan, Inkyu Shin, Francois Rameau, Seokju Lee, and In So Kweon. Unsupervised intra-domain adaptation for semantic segmentation through self-supervision. *arXiv preprint arXiv:2004.07703*, 2020. [6](#), [7](#)
- [39] Marie-Morgane Paumard, David Picard, and Hedi Tabia. Image reassembly combining deep learning and shortest path problem. In *Proceedings of the European Conference on Computer Vision (ECCV)*, pages 153–167, 2018. [2](#)
- [40] Kuniaki Saito, Donghyun Kim, Stan Sclaroff, Trevor Darrell, and Kate Saenko. Semi-supervised domain adaptation via minimum entropy. In *Proceedings of the IEEE International Conference on Computer Vision*, pages 8050–8058, 2019. [2](#), [5](#), [6](#), [7](#), [8](#)
- [41] Kuniaki Saito, Yoshitaka Ushiku, Tatsuya Harada, and Kate Saenko. Adversarial dropout regularization. *arXiv preprint arXiv:1711.01575*, 2017. [2](#)
- [42] Kuniaki Saito, Kohei Watanabe, Yoshitaka Ushiku, and Tatsuya Harada. Maximum classifier discrepancy for unsupervised domain adaptation. In *Proceedings of the IEEE Conference on Computer Vision and Pattern Recognition*, pages 3723–3732, 2018. [2](#)
- [43] Fatemeh Sadat Saleh, Mohammad Sadegh Aliakbarian, Mathieu Salzmann, Lars Petersson, and Jose M Alvarez. Effective use of synthetic data for urban scene semantic segmentation. In *European Conference on Computer Vision*, pages 86–103. Springer, 2018. [2](#)
- [44] Swami Sankaranarayanan, Yogesh Balaji, Arpit Jain, Ser Nam Lim, and Rama Chellappa. Learning from synthetic data: Addressing domain shift for semantic segmentation. In *Proceedings of the IEEE Conference on Computer Vision and Pattern Recognition*, pages 3752–3761, 2018. [1](#), [2](#)
- [45] Rodrigo Santa Cruz, Basura Fernando, Anoop Cherian, and Stephen Gould. Deeppermnet: Visual permutation learning. In *Proceedings of the IEEE Conference on Computer Vision and Pattern Recognition*, pages 3949–3957, 2017. [2](#)
- [46] Dror Sholomon, Omid David, and Nathan Netanyahu. A generalized genetic algorithm-based solver for very large jigsaw puzzles of complex types. In *Proceedings of the AAAI Conference on Artificial Intelligence*, volume 28, 2014. [2](#)
- [47] Yi-Hsuan Tsai, Wei-Chih Hung, Samuel Schulter, Kihyuk Sohn, Ming-Hsuan Yang, and Manmohan Chandraker. Learning to adapt structured output space for semantic segmentation. In *Proceedings of the IEEE Conference on Computer Vision and Pattern Recognition*, pages 7472–7481, 2018. [1](#), [2](#), [3](#), [6](#)
- [48] Yi-Hsuan Tsai, Kihyuk Sohn, Samuel Schulter, and Manmohan Chandraker. Domain adaptation for structured output via discriminative patch representations. In *Proceedings of the IEEE International Conference on Computer Vision*, pages 1456–1465, 2019. [2](#), [3](#)
- [49] Eric Tzeng, Judy Hoffman, Kate Saenko, and Trevor Darrell. Adversarial discriminative domain adaptation. In *Proceedings of the IEEE Conference on Computer Vision and Pattern Recognition*, pages 7167–7176, 2017. [1](#), [2](#)
- [50] Hemant Venkateswara, Jose Eusebio, Shayok Chakraborty, and Sethuraman Panchanathan. Deep hashing network for unsupervised domain adaptation. In *Proceedings of the*

*IEEE conference on computer vision and pattern recognition*, pages 5018–5027, 2017. 5

- [51] Tuan-Hung Vu, Himalaya Jain, Maxime Bucher, Matthieu Cord, and Patrick Pérez. Advent: Adversarial entropy minimization for domain adaptation in semantic segmentation. In *Proceedings of the IEEE Conference on Computer Vision and Pattern Recognition*, pages 2517–2526, 2019. 1, 2, 3, 6
- [52] Yanchao Yang and Stefano Soatto. Fda: Fourier domain adaptation for semantic segmentation. In *Proceedings of the IEEE/CVF Conference on Computer Vision and Pattern Recognition*, pages 4085–4095, 2020. 2, 6
- [53] Ting Yao, Yingwei Pan, Chong-Wah Ngo, Houqiang Li, and Tao Mei. Semi-supervised domain adaptation with subspace learning for visual recognition. In *Proceedings of the IEEE conference on Computer Vision and Pattern Recognition*, pages 2142–2150, 2015. 2
- [54] Jingyi Zhang, Jiaxing Huang, Zhipeng Luo, Gongjie Zhang, and Shijian Lu. Da-detr: Domain adaptive detection transformer by hybrid attention. *arXiv preprint arXiv:2103.17084*, 2021. 2
- [55] Xiaobing Zhang, Haigang Gong, Xili Dai, Fan Yang, Nianbo Liu, and Ming Liu. Understanding pictograph with facial features: End-to-end sentence-level lip reading of chinese. In *AAAI*, pages 9211–9218, 2019. 2
- [56] Yang Zhang, Philip David, and Boqing Gong. Curriculum domain adaptation for semantic segmentation of urban scenes. In *Proceedings of the IEEE International Conference on Computer Vision*, pages 2020–2030, 2017. 2
- [57] Zhun Zhong, Liang Zheng, Zhiming Luo, Shaozi Li, and Yi Yang. Invariance matters: Exemplar memory for domain adaptive person re-identification. In *Proceedings of the IEEE Conference on Computer Vision and Pattern Recognition*, pages 598–607, 2019. 2
- [58] Yang Zou, Zhiding Yu, Xiaofeng Liu, BVK Kumar, and Jinsong Wang. Confidence regularized self-training. In *Proceedings of the IEEE International Conference on Computer Vision*, pages 5982–5991, 2019. 2, 6
- [59] Yang Zou, Zhiding Yu, BVK Vijaya Kumar, and Jinsong Wang. Unsupervised domain adaptation for semantic segmentation via class-balanced self-training. In *Proceedings of the European Conference on Computer Vision (ECCV)*, pages 289–305, 2018. 2